Am. J. Trop. Med. Hyg., 93(4), 2015, pp. 875–890
doi:10.4269/ajtmh.15-0330

Modeling the Present and Future Geographic Distribution of the Lone Star Tick, *Amblyomma americanum* (Ixodida: *Ixodidae*), in the Continental United States

Yuri P. Springer,* Catherine S. Jarnevich, David T. Barnett, Andrew J. Monaghan, and Rebecca J. Eisen

Division of Vector-Borne Diseases, Centers for Disease Control and Prevention, Fort Collins, Colorado; U.S. Geological Survey, Fort Collins, Colorado; National Ecological Observatory Network, Inc., Boulder, Colorado; National Center for Atmospheric Research, Boulder, Colorado

Abstract. The Lone star tick (*Amblyomma americanum* L.) is the primary vector for pathogens of significant public health importance in North America, yet relatively little is known about its current and potential future distribution. Building on a published summary of tick collection records, we used an ensemble modeling approach to predict the present-day and future distribution of climatically suitable habitat for establishment of the Lone star tick within the continental United States. Of the nine climatic predictor variables included in our five present-day models, average vapor pressure in July was by far the most important determinant of suitable habitat. The present-day ensemble model predicted an essentially contiguous distribution of suitable habitat extending to the Atlantic coast east of the 100th western meridian and south of the 40th northern parallel, but excluding a high elevation region associated with the Appalachian Mountains. Future ensemble predictions for 2061–2080 forecasted a stable western range limit, northward expansion of suitable habitat into the Upper Midwest and western Pennsylvania, and range contraction along portions of the Gulf coast and the lower Mississippi river valley. These findings are informative for raising awareness of *A. americanum*-transmitted pathogens in areas where the Lone Star tick has recently or may become established.

INTRODUCTION

One of the most widely anticipated ecological effects of climate change involves the geographic redistribution of organisms.[1] There is growing evidence that as temperatures increase globally, the ranges of many species will expand or shift into higher latitudes and elevations as organisms track their current thermal or abiotic niche.[2–4] This phenomenon may be especially pronounced for ectothermic taxa and those for which temperature and associated abiotic conditions play critical roles in regulating physiological or ecological processes.[5,6] Terrestrial arthropods meet these criteria and have been the focus of considerable attention in this regard because many species play central roles in the transmission of wildlife, livestock, and human pathogens.[7–9] Changes in the geographic distribution and abundance of vector species driven by climate change may thus have significant consequences for the incidence and biogeography of infectious diseases.[10–15] In light of this possibility, there is a growing need to accurately predict changes in the distribution of arthropod vector species under future climate change scenarios.

Among vector taxa, climate impacts on the biogeography of ticks and tick-borne pathogens are of particular concern for at least two reasons. First, ticks transmit a greater variety of parasites and pathogens than any other biting arthropod[16] and are responsible for the vast majority of vector-borne infections of humans in northern temperate latitudes.[17,18] Tick-borne pathogens also cause some of the most common and economically important diseases of livestock, especially cattle.[19,20] Second, ticks are likely to shift their geographic distribution in response to climate change because they are highly sensitive to temperature and humidity, which are expected to change over time. Physiological constraints associated with temperature and humidity are known to have profound effects on the growth, survival, and reproduction of ticks.[21–23] As a result, temperature and humidity significantly influence patterns of tick distribution and abundance.[24,25] By extension, it seems very likely that large-scale changes in these conditions could give rise to changes in tick biogeography. Indeed, data from Europe and North America provide evidence that tick distributions have recently shifted or expanded into higher latitudes and altitudes in parallel with rising temperatures.[26–29] Although mechanisms other than climate variability and change undoubtedly contribute to these outcomes,[30] the repeated observation of range changes correlated with temperature, in a manner consistent with known physiological constraints, argues strongly for a central role of climate in driving changes in tick distributions at broad geographic scales.[31–33] This recognition, and the aforementioned agricultural and public health significance of ticks, underlie a growing interest in tick distribution modeling based on future climate scenarios.[34–37] Predictions of these models may provide valuable forecasts of changing acarological risk associated with tick-borne diseases that could be used to inform vector monitoring and control efforts and public health campaigns.

Bioclimatic envelope modeling, also known as ecological niche or habitat suitability modeling, describes a suite of methods developed in part to enable predictions of how climate change may affect organismal range limits.[38–40] The general approach, predicated on basic niche theory,[41,42] involves two steps. First, inferences are made about the fundamental niche of a focal species (here, the abiotic conditions under which viable populations are likely to be maintained) using measured physiological thresholds or, more commonly, data on the species' current distribution and environmental conditions in areas of occurrence. Correlational relationships between range limits and preferred or tolerated climatic conditions are thereby identified, though in reality these may be more closely tied to the realized rather than the fundamental niche. Second, future climate predictions are used to quantify how the geographic distribution of these conditions, and associated distributional limits of the focal species, might change in the future. This approach has been criticized for various

*Address correspondence to Yuri P. Springer, Division of Vector-Borne Diseases, Centers for Disease Control and Prevention, 3150 Rampart Road, Fort Collins, CO 80521. E-mail: yurispringer@gmail.com

shortcomings including its failure to incorporate biotic interactions, dispersal, and evolutionary dynamics.[43,44] Nevertheless, there is general agreement and growing empirical support for the conjecture that at relatively large spatial scales, climatic relationships make significant contributions to, and may determine, distributional limits.[40,45] Although some limitations to the approach are difficult to overcome (e.g., availability of both presence and confirmed absence data), recent improvements in predictive quality have been achieved through the use of ensemble modeling approaches that synthesize outputs of multiple predictive models that vary in their assumptions and algorithms.[46,47]

Here, we use bioclimatic modeling and climate change forecasts to predict the potential geographic distribution of localities anticipated to be suitable for establishment of the Lone star tick, *Amblyomma americanum* within the continental United States. Considered a major nuisance biter,[48–50] *A. americanum* is also increasingly recognized as one of the most important tick vectors in North America. Pathogens transmitted by the Lone star tick are known to infect both humans and domestic animals and include multiple species in the genera *Rickettsia* (e.g., *Rickettsia rickettsia, Rickettsia parkeri*) and *Ehrlichia* (e.g., *Ehrlichia chaffeensis, Ehrlichia ewingii*), *Francisella tularensis*, and Heartland virus.[51–55] In spite of its significant impacts on wildlife, livestock, and human health, relatively little is known about the current and potential future distribution of *A. americanum*. Building on a published summary of tick collection records reported from 1898 to 2012,[56] we use an ensemble approach involving five different algorithms to model the current distribution of localities climatically suitable for establishment of the Lone star tick (hereafter suitable habitat) in the continental United States. By integrating multiple algorithms, ensemble modeling reduces the potential for predictive bias that may arise when only a single algorithm is considered. We then use insights obtained through this exercise, including the climatic variables and conditions associated with the tick's current distribution, to predict the future geographic distribution of suitable tick habitat under two greenhouse gas (GHG) emissions scenarios using five general circulation models.

MATERIALS AND METHODS

Tick distribution data. We used published data on the geographic distribution of *A. americanum* collection records in the United States as the basis of our modeling.[56] These data were generated by compiling Lone star tick collection records obtained from a search of the published literature and databases managed by the U.S. Department of Agriculture, U.S. National Tick Collection, and Walter Reed Biosystematics Unit. A total of 18,121 *A. americanum* collection records, involving sampling events conducted at locations across the continental United States (48 states and the District of Columbia, hereafter DC) and reported from 1898 to 2012, were summarized at the county level. Using a threshold described by Dennis and others,[57] *A. americanum* was categorized as "established" in a county if six or more ticks, or two or more life stages, were associated with one or more collection records in a single year. The species was categorized as "reported" if the number of specimens or life stages collected did not exceed these thresholds or was not specified. The remaining counties had "no records" and were categorized as such.

On the basis of these data, Springer and others[56] categorized *A. americanum* as established in 653 counties distributed across 32 states and the DC (Supplemental Table 1 Figure 1A).[56] In our analyses, we excluded two of these counties from our list of those classified as present (Ravalli county, Montana and Sacramento county, California) because they fall far outside of the geographic core of the species' distribution and associated collections were likely the result of importation rather than sampling of locally established populations. In addition, while Springer and others[56] categorized *A. americanum* as reported in an additional 647 counties, we classified the species as absent from these locations in our analyses. Because these collection records reflect where efforts were made to sample or study ticks, the geographic distribution of *A. americanum* inferred from these data, and that forms the basis of our analyses, likely underestimates the species' true current distribution. Although the inferred distribution consists of both present locations (651 established counties) and presumed absence locations (2,458 reported and no records counties), we have greater confidence in the former than the latter. Given this, we ran the species distribution models using all non-presence counties as background to characterize available environment rather than as presence/absence models that contrast environmental conditions associated with presence and absence locations.

Selecting and quantifying climate predictor variables. Climate predictor variables included in our present-day distribution modeling were drawn from four sets. The first set consisted of the 19 standard bioclimatic variables available at 2.5 arc minutes resolution from version 1.4 of WorldClim.[58] WorldClim is a set of global climate layers based on interpolations of temperature and precipitation from weather stations around the globe, averaged across the years between 1950 and 2000. For the second set, we calculated multiple estimates of growing degree days (GDDs), a predictor variable identified as important in a number of previous models of tick-associated phenomena.[25,59,60] We estimated daily GDDs from monthly WorldClim temperature data that were calibrated with daily data obtained from Daymet[61] (calculation methods described in Supplemental Material 1). This resulted in 23 variables associated with growing degree days: mean number of GDDs for each month and cumulative from the start of the year for each month (monthly and cumulative values are identical for the month of January). To generate the third and fourth variable sets, we calculated monthly average values for vapor pressure (a measure of humidity) and number of days with snow cover (based on the presence of snow inferred from values of snow water equivalent > 0) using data for the period 1980–2000 available from Daymet.[62] This generated an additional 24 variables, bringing the total number of climate predictor variables considered for possible inclusion in our present-day distribution modeling to 66. Because our tick distribution data had county-level spatial resolution, we used the Zonal Statistics tool in ArcGIS version 10.2 (Environmental Systems Resource Institute, 2010; ESRI, Redlands, CA) to calculate a county-level mean value for each of the 66 historical climate predictor variables. Means for each county were calculated using data from every 2.5 arc minutes climate data grid cell whose centroid fell inside the county boundary.

Future climate data underpinning our predictions of the future geographic distribution of suitable habitat were derived

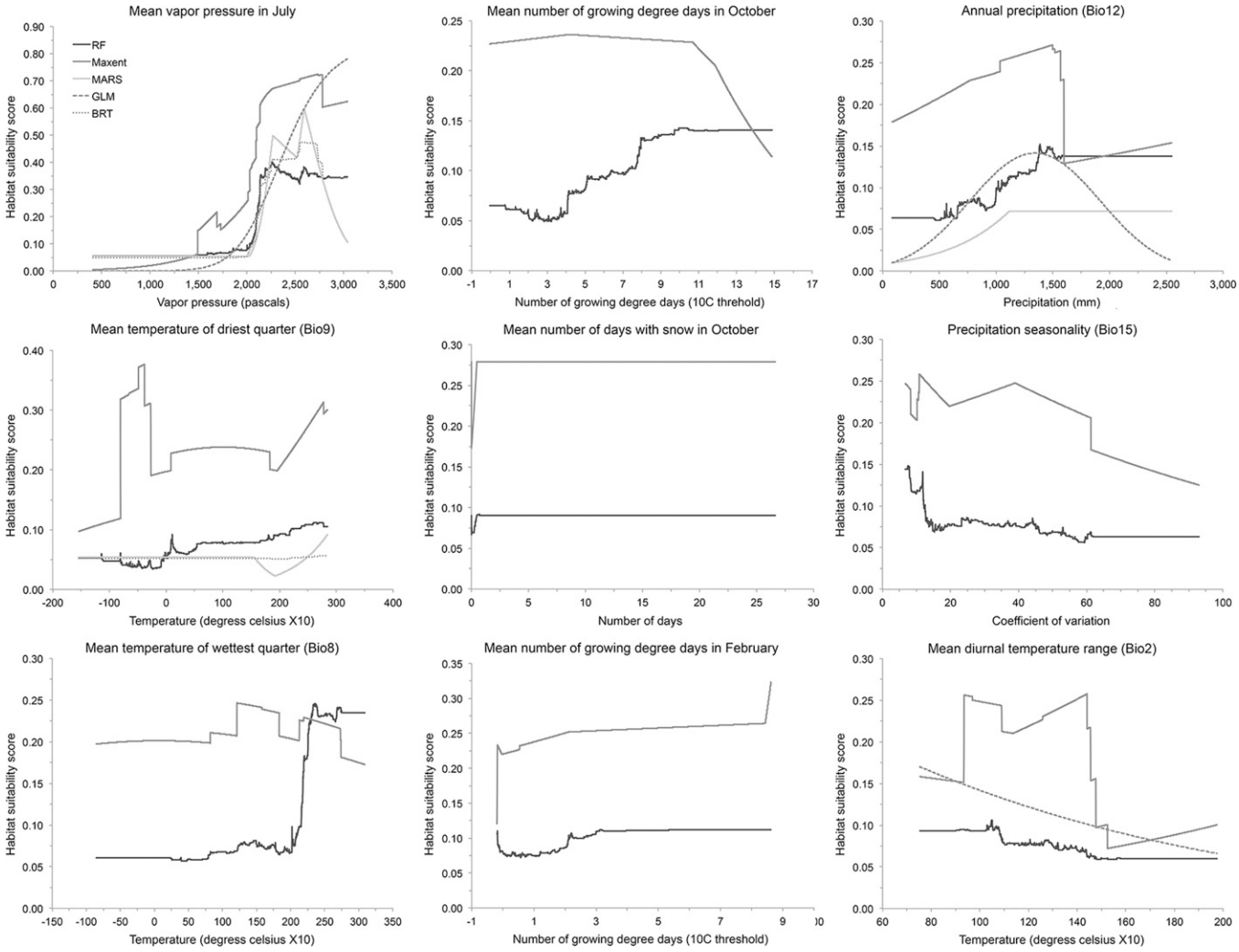

FIGURE 1. Response curves for the climate predictor variables that comprised the reduced set included in the optimized models. In each of the figures, the *x* axis depicts the range of observed values for each climate predictor variable in the full training dataset and the y axis indicates the associated habitat suitability scores (0 = not suitable, 1 = maximum suitability).

using empirically downscaled projections from five Atmosphere Ocean General Circulation Models (AOGCMs) that support phase five of the Coupled Model Intercomparison Experiment (CMIP5).[64] Multiple AOGCMs were used to reduce uncertainty due to differences among climate models (e.g., because of the way they each represent various processes, their spatial resolution, etc.). The five AOGCMs were chosen based on two criteria. First, each model is available in the WorldClim database at 2.5 arc minutes resolution and is thus consistent with scale of the historical WorldClim data described above. Second, each model ranks among the top of the CMIP5 AOGCMs in its ability to simulate observed temperature and rainfall globally.[65] The following five AOGCMs were chosen: 1) version 4 of the Community Climate System Model (CCSM4),[66] 2) the low-resolution version of the Max Planck Institute Earth System Model (MPI-ESM-LR),[67] 3) the full-earth-system version of the Met Office Hadley Center second generation family of coupled climate models (HadGEM2-ES),[68] 4) CNRM-CM5,[69] and 5) ACCESS1-0.[70] Details on the AOGCM downscaling methodology are available at http://worldclim.org/downscaling.

We used the future climate projections for 2061–2080 from two Representative Concentration Pathway (RCP) emissions scenarios,[71] RCP4.5 and RCP8.5. Two RCP scenarios were used to incorporate uncertainty in future climate change that results from the unknown GHG emissions trajectory that humanity will take. RCP8.5 is a high-emissions scenario with GHG radiative forcing reaching 8.5 W/m^2 near 2,100. It represents a plausible trajectory if little is done to curb GHG emissions.[72] RCP4.5 is a low-to-moderate emissions scenario with GHG radiative forcing reaching 4.5 W/m^2 near 2,100, without ever exceeding the value. It represents a trajectory that may be plausible if, for instance, GHG emissions pricing were introduced to limit radiative forcing.[73]

On the basis of results of our present-day distribution modeling, only three climate predictor variables were associated with our predictions of future habitat suitability. Two were among the 19 standard WorldClim bioclimatic variables (mean diurnal temperature range [Bio2] and annual precipitation [Bio12]), and predicted future values of these variables were downloaded directly from WorldClim. Values of the third variable, mean vapor pressure in July, were calculated

from historical values of vapor pressure (from Daymet) and both historical and future mean temperature (from WorldClim) (calculation methods described in Supplemental Material 2). Vapor pressure that quantifies the partial pressure of water vapor in the atmosphere, is a temperature-dependent measure of humidity. Vapor pressure is related to a better known humidity variable, relative humidity (RH) that is the ratio of the "actual" measured vapor pressure to the "saturated" vapor pressure (the partial pressure of water vapor at which an air parcel at a given temperature will become saturated). Knowing this ratio and assuming future RH remains constant at historical values, future vapor pressure can be calculated. The assumption of constant RH in the future is consistent with studies based on observations of historical change and AOGCM results.[74,75] Notably, this means that the future vapor pressure will be higher, because more water vapor is required to achieve saturation (i.e., a RH of 100%) under warmer conditions.

Modeling present-day distribution. Before beginning the present-day distribution modeling, we first evaluated all pairwise correlations among the 66 climate predictor variables to minimize statistical issues associated with colinearity. We generated a matrix that listed the largest value from among three correlation coefficients (Pearson, Spearman, and Kendall) calculated for each pair of variables. To choose variables from among the full set of 66 to include in the present-day distribution modeling, we first listed the variables in descending order by their respective values of deviance explained. This parameter serves as an analog of R-squared in a general additive model (GAM) and here, estimates the amount of variation in the present-day distribution of *A. americanum* explained by a given climate predictor variable.[76] It is calculated from a univariate GAM function fit to the presence/background data for the tick and associated values of the climate predictor variable. From the ordered list of variables, we selected the one with the highest value of deviance explained to include in the reduced set and then manually went down the list, considering each successive variable for inclusion in the reduced set based on its pairwise correlation with the variable(s) already selected. A given variable was added to the reduced set if none of its pairwise correlations with variables already in the reduced set exceeded ±0.7 in magnitude.[77] Unless otherwise noted, all statistical analyses were performed using VisTrails Software for Assisted Habitat Modeling (SAHM).[78]

We modeled the present-day distribution of suitable habitat within the continental United States using all five algorithms available in SAHM: 1) boosted regression trees (BRTs),[79] 2) generalized linear models (GLMs),[80] 3) multivariate adaptive regression splines (MARSs),[81] 4) maximum entropy (Maxent),[82] and 5) random forests (RFs).[83] Each of these algorithms performs well with presence/background data, and because algorithm selection represents the greatest source of quantifiable uncertainty in model predictions,[84] consideration of multiple algorithms allowed us to evaluate and reduce the potential biasing effects of algorithm choice on our results. Inputs to each model included county-level tick status (present [N = 651 counties] or background [N = 2,458]) and values for each climate predictor variable in the reduced set. As described above, we used the Zonal Statistics tool in ArcGIS version 10.2 to calculate a county-level mean value for each climate predictor variable. On the basis of this input information, each model identified a unique, algorithm-specific set of climate conditions associated with locations where *A. americanum* was classified as present. In the present-day distribution models, these correlations underlie predictions of locations where *A. americanum* may be currently established based on the presence of climate conditions favorable for tick survival.

Construction of the five present-day distribution models used the 10-fold cross-validation method. After first running each model with the full location dataset including all presence and background counties (training run), we randomly divided the dataset into 10 equal subsets and ran the model an additional 10 times, withholding one subset during each run (testing runs). Each of the 11 runs of each model generated a continuous habitat suitability score (range = 0–1) for each county. For each run, the value of the continuous habitat suitability score that maximized the sum of sensitivity and specificity was calculated and used as a threshold to convert the continuous score into a binary habitat suitability score that classified each county as either suitable (score = 1) or unsuitable (score = 0).[85,86] These binary scores formed the basis of the associated confusion matrix.

We evaluated and optimized the fit (performance) of each present-day distribution model using multiple, SAHM-generated metrics of agreement between the predicted and observed county-level tick distributions generated by the training and/or testing runs. First, we examined receiver operating characteristic (ROC) curves and associated values for area under the curve (AUC)[87] for training and testing runs. When the difference between the training AUC and the mean of the testing AUC values exceeded 0.05, we ran several iterations of the model, adjusting default parameter settings to identify the iteration with optimized performance (i.e., smallest difference in AUC scores and minimal overfitting as assessed by visual examination of response curves for each climate predictor variable). If multiple iterations of a model had similar performance as measured by this ROC/AUC-based criterion, we distinguished them based on values of several metrics of fit derived from their confusion matrices including the true skill statistic (TSS, a modified Kappa statistic that accounts for and reflects rates of omission and commission errors but is not sensitive to prevalence),[88] correlation coefficient (between observed and predicted values), percent correctly classified (the percent of counties correctly classified by the model relative to known establishment/presumed absence of *A. americanum)*, and deviance explained (R-squared analog). We selected as optimal the model iteration with the highest relative values of these metrics. Once selected, we performed testing and training runs using this optimal model and used these as our final optimized model in all subsequent analyses. BRT models with default settings appeared overfit, and we optimized parameters following Elith and others,[79] selecting tree complexity of two, learning rate of 0.005, and 5,000 trees where response curves were smoothed while maintaining high performance metrics with minimized difference between training data and testing data calculations.

Predicting future distribution. We predicted the future distribution of suitable habitat within the continental United States using the optimized present-day distribution model constructed with the GLM algorithm. Compared with models derived from the other four algorithms, GLM-derived models tend to be relatively simple in their structure, making them less sensitive to spurious results that may arise during the extrapolation involved in future projections and thus more appropriate for capturing the potential rather than realized

niche.[89] We applied the GLM model 10 times, using as inputs the predicted future county-level climate conditions associated with each unique combination of AOGCM ($N = 5$) and RCP ($N = 2$). As in the present-day modeling, each model application (AOGCM/RCP combination) generated a continuous habitat suitability score that we converted to a binary score (suitable/unsuitable) using the aforementioned threshold value. Using SAHM, we calculated the Multivariate Environmental Similarity Surface (MESS) for each model application to highlight counties where prediction uncertainty was high. The MESS identifies areas where the future value of a given climate predictor variable forecasted by the AOGCM is more extreme than any value for that variable in the present-day training dataset. These areas of extrapolation represent locations for which future predictions should be made with greater caution. Each county was assigned a MESS score that indicated whether predicted future climatic conditions did (score = 1) or did not (score = 0) fall outside the range of historically observed conditions.

Visualization and evaluation of present-day modeling results. For results of our present-day distribution modeling, we quantified the relative contribution of climate predictor variables in the reduced set to each of the five optimized present-day distribution models (hereafter optimized models) using metrics generated in SAHM. The number and identity of included variables differed among optimized models. To evaluate the relative contribution of a given variable to a model, SAHM randomized values of the variable among counties relative to tick status (present, background) and calculated a model AUC. The magnitude of the difference between this AUC score and that of the original optimized model, termed the train contribution value, is positively related to the explanatory power of the climate predictor variable for which values were randomized. To facilitate comparisons among variables within and across optimized models we normalized train contribution values by converting them to percentages across all variables within each model. In addition, we examined the shape of the response curves for each climate predictor variable across all optimized model in which it was included. These curves graphically depict the relationship between values of the variable and habitat suitability as predicated by the different models. More broadly, we quantified the overall performance (fit) of each optimized model using multiple metrics generated in SAHM. In addition to those previously mentioned (AUC score, TSS, correlation coefficient, percent correctly classified, deviance explained), these included sensitivity (the proportion of established counties classified as presence locations by the model) and mean threshold (value used to dichotomize the continuous model output into the threshold-dependent binary matrix). We did not report specificity since counties classified as background represented presumed rather than confirmed absence locations. For each of the five optimized models, values for each performance metric were generated for both the training run (full location dataset including all presence and background counties) and as an average across all 10 testing runs.

Using results associated with the five optimized models, we created an ensemble model[46] to predict the present-day distribution of suitable habitat within the continental United States. This was accomplished by adding together the binary habitat suitability score maps of all optimized models that had an average testing AUC value > 0.7, biologically realistic response curves, and acceptably high values for metrics of fit derived from the confusion matrix. Thus, in our ensemble model, each county was associated with a consensus habitat suitability score (range = 0–5) indicating the number of five optimized models that classified it as representing suitable habitat. To evaluate predictions of the ensemble model, we compared these consensus habitat suitability scores to categorization made by Springer and others[56] based on tick collection records (established, reported, no records). We also created a map of the continuous habitat suitability scores generated by each model to visualize how specific underlying predictions of individual models differed from those of the ensemble model.

Visualization and evaluation of future predictions. As with the present-day modeling, we created ensemble maps for use in predicting the future distribution of suitable habitat within the continental United States. To produce these for each of the two RCPs, we added together the binary habitat suitability score maps of all five GLM-based AOGCM future predictions. This generated an ensemble prediction in which each county was associated with a consensus habitat suitability score (range = 0–5). A score of 0 indicates that none of the five AOGCMs forecasted that the county in question would experience climatic conditions associated with suitable habitat (i.e., matching the climatic conditions found in locations where the tick is currently established). We compared consensus habitat suitability scores underlying the present-day and future ensemble maps to identify areas where forecasted changes in climatic conditions are predicted to alter habitat suitability (i.e., potential areas of range expansion or contraction). To evaluate uncertainty in our future predictions, we created an ensemble MESS map for each of the two ensemble prediction maps by summing MESS scores across the five GLM-based AOGCM future predictions. Each county was thereby assigned a consensus MESS score (range = 0–5). A score of 0 indicates that climatic conditions predicted in the county in question did not fall outside the range of historically observed conditions in any of the five AOGCMs (i.e., no extrapolation, high confidence). In contrast, a score of 5 indicates that predicted climatic conditions fell outside the range of historically observed conditions in all five AOGCMs (i.e., extensive extrapolation, low confidence).

RESULTS

Selecting and quantifying climate predictor variables. Using the correlation matrix, we reduced our original set of 66 climate predictor variables down to a reduced set of nine variables (Table 1). Among optimized models, the number of variables included and their relative importance to the models varied (Table 1). Notably, mean vapor pressure in July was the only variable included in all five optimized models and had the highest normalized train contribution value in each model (≥ 69.99); across all models, its average train contribution value was over 11 times greater than that of the variable with the second highest explanatory power. Mean temperature of the driest quarter (Bio9) and annual precipitation (Bio12) were included in four of the five models, but normalized train contribution values were less than 10.07.

All of the optimized models performed well, with mean test AUC scores between 0.82 and 0.86 (Table 2). Across the full dataset, the percent of counties correctly classified by the

TABLE 1

Performance statistics associated with each of the nine climate predictor variables in the reduced set used in our present-day distribution modeling. For each variable, the value of deviance explained is parenthetically accompanied by the rank of this value in the list of values for all 66 of the originally considered climate predictor variables, arranged in descending order (i.e., a rank of 1 indicates the highest value). Also provided are the normalized train contribution values for each variable in each of the five optimized models. A blank cell indicates that the variable was not included in the corresponding optimized model. Variables obtained from WorldClim have their associated Bioclim labels indicated parenthetically

Climate predictor variable	Deviance explained (rank)	Normalized train contribution values				
		BRT	GLM	MARS	Maxent	RF
Mean vapor pressure in July	26.13 (1)	92.80	93.10	84.21	69.99	76.39
Mean number of growing degree days in October	10.09 (34)	–	–	–	1.09	2.98
Annual precipitation (Bio12)	10.07 (35)		4.54	9.42	1.70	3.81
Mean temperature of driest quarter (Bio9)	8.57 (42)	7.20	–	6.38	10.04	6.18
Mean number of days with snow in October	6.21 (50)	–	–	–	0.99	0.06
Precipitation seasonality (Bio15)	4.91 (54)	–	–	–	5.03	3.92
Mean temperature of wettest quarter (Bio8)	2.13 (61)	–	–	–	3.30	3.09
Mean number of growing degree days in February	1.74 (62)	–	–	–	1.12	0.61
Mean diurnal temperature range (Bio2)	1.15 (64)		2.35	–	6.73	2.98

BRT = boosted regression tree; GLM = generalized linear model; MARS = multivariate adaptive regression spline; Maxent = maximum entropy; RF = random forest.

models (relative to the known establishment or presumed absence of A. americanum based on Springer and others[56]) ranged from 71% to 75%. More specifically, the proportion of established counties classified by the models as "present" locations was at least 0.89 in every model. Values of the other performance statistics reinforced the conclusion that the fits of the optimized models were good overall. Because the models were built assuming presence/background data, output values (continuous habitat suitability scores) were not directly comparable across models. This necessitated the conversion to binary scores that could be combined to create the ensemble model. In evaluating approaches to combining scores, Marmion and others[90] found that the highest performing method involved weighting binary scores based on the AUC of the associated model. This was our method of choice, but because the AUC scores of our five models were so similar we opted to forgo any weighting. Further, because the five models all performed comparably (Table 2) yet differed in terms of the climate predictor variables they included and the geographic patterns of continuous habitat suitability scores they predicted (Figure 2C–G), we concluded that each would make a unique contribution to and warranted inclusion in the ensemble model.

Predictor variable response curves. Plots of the response curves for the climate predictor variables illustrated that the relationships between mean vapor pressure in July and habitat suitability had a fairly consistent shape among optimized models, with indications of a minimum threshold value between 1,500 and 2,000 Pa (Figure 1). Curves associated with at least three of the five models further suggested that maximum habitat suitability was achieved when values for mean vapor pressure in July were between 2,250 and 2,750 Pa, with declining habitat suitability at higher pressures. The shapes of the response curves for mean temperature of driest quarter (Bio9) varied among models, with relatively flat curves for the BRT and MARS models, a nearly flat curve showing very slight increases in habitat suitability above 5°C for the RF model, and an erratic curve for the Maxent model with highest habitat suitability corresponding to temperatures between −8 and −4°C and lower but relatively constant suitability between 0 and 17.5°C. Response curves for annual precipitation (Bio12) indicated a positive relationship between habitat suitability and annual precipitation up to a maximum between 1,200 and 1,400 mm, with either no further increases or declines in suitability at higher precipitation values. Two of three curves for mean diurnal temperature range (Bio2) showed a slight negative relationship, with the highest values of habitat suitability associated with temperature range values of 9 to 11°C. As was the case with mean temperature of driest quarter, the curve associated with the Maxent model was erratic and indicated relatively high habitat suitability for a mean diurnal temperature range from 9 to 14°C, with a precipitous decline at ranges above 14°C. Relative to the curves generated for the other four models, those associated with the optimized GLM-based model were comparatively smooth, providing evidence of the model's simple structure and low sensitivity to spurious correlations in the data. Further, the general shapes of the GLM-associated curves were consistent with relationships between climatic conditions and habitat

TABLE 2

Values of multiple performance metrics associated with each of the five optimized models. For each model, metric values are provided for both the training run (full location dataset including all presence and background counties) and as an average across all 10 testing runs

Performance metric	BRT		GLM		MARS		Maxent		RF	
	Test split	Train	Test split	Train	Test split	Train	Test split	Train	Test split	Train
AUC	0.83	0.84	0.82	0.82	0.82	0.83	0.84	0.87	0.86	0.86
True skill statistic	0.55	0.57	0.54	0.56	0.55	0.56	0.56	0.61	0.45	0.59
Correlation coefficient	0.48	0.50	0.46	0.47	0.46	0.48	0.47	0.50	0.54	0.54
Percent correctly classified	72.13	72.51	70.36	70.78	71.04	70.68	74.01	75.17	82.07	72.80
Deviance explained (percent)	23.39	24.92	23.02	24.16	23.56	24.89	8.35	9.35	30.19	29.40
Sensitivity	0.87	0.89	0.89	0.91	0.88	0.90	0.84	0.90	0.56	0.91
Mean threshold	0.27	0.29	0.21	0.20	0.16	0.12	0.55	0.57	0.43	0.16

AUC = area under the curve; BRT = boosted regression tree; GLM = generalized linear model; MARS = multivariate adaptive regression spline; Maxent = maximum entropy; RF = random forest.

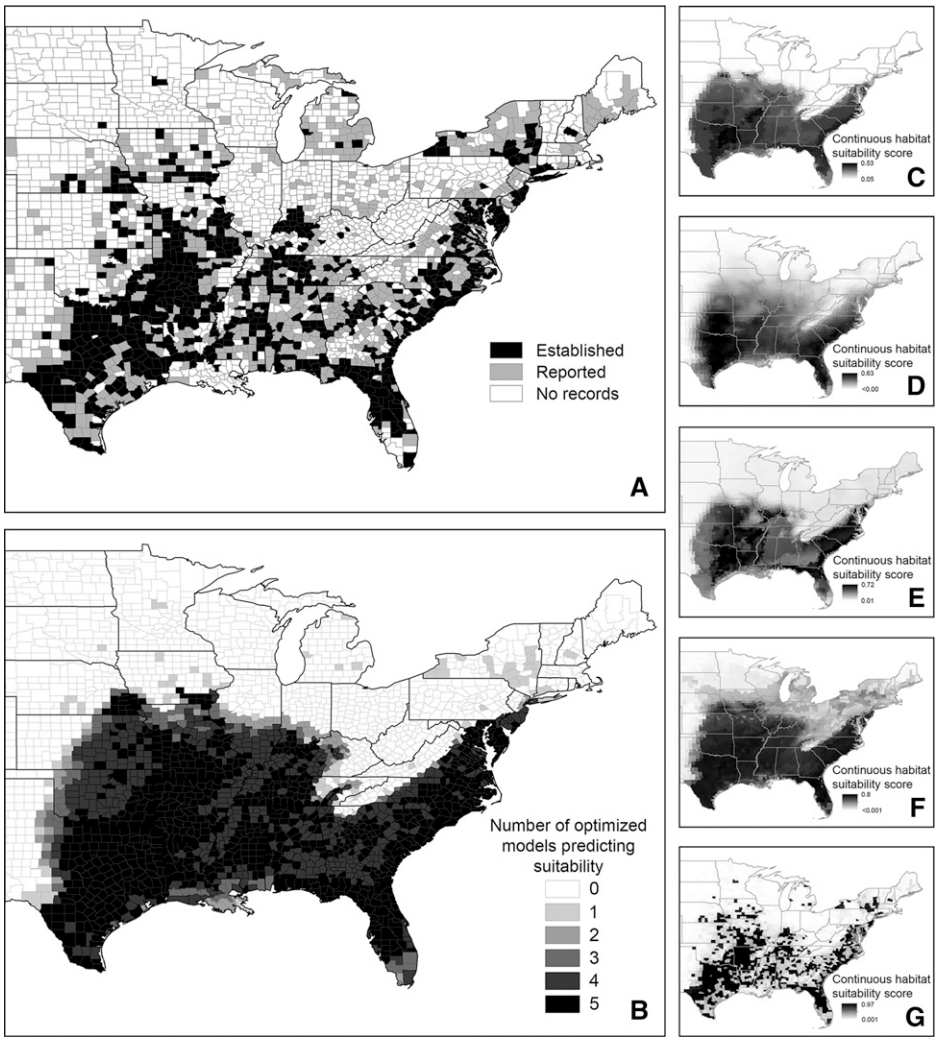

FIGURE 2. Maps depicting *Amblyomma americanum* collection records and results of the present-day distribution modeling. (**A**) County-level classification of *A. americanum* collection records, cumulative from 1898 through 2012 (established, reported, no records), based on Springer and others.[56] (**B**) Map of present-day ensemble model depicting consensus habitat suitability scores. Scores indicate the number of the five optimized models that classified a given county as having climatic conditions suitable for the establishment of *A. americanum*. (**C–G**) Maps depicting the continuous habitat suitability scores predicted by each of the individual optimized models: BRT, GLM, MARS, Maxent, and RF, respectively. BRT = boosted regression tree; GLM = generalized linear model; MARS = multivariate adaptive regression spline; Maxent = maximum entropy; RF = random forest.

suitability for ticks that would be expected based on fundamental aspects of tick physiology and ecology.

Visualization and evaluation of present-day modeling results. The pattern of distribution of suitable habitat shown in the present-day ensemble map (Figure 2B) was largely consistent with the map of county-level collection records of *A. americanum* (Figure 2A) generated by Springer and others.[56] The ensemble map projected a relatively contiguous swath of counties categorized as suitable habitat beginning at roughly the intersection of the 100th western meridian (hereafter 100th meridian), which forms the eastern border of the Texas panhandle with Oklahoma, and the 40th northern parallel (hereafter 40th parallel), which is coincident with border of Kansas with Nebraska. In the collection records map, this area is associated with the majority of counties categorized as established but also with many counties categorized as reported or associated with no collection records. Assuming that *A. americanum* is indeed established across much or all of this area, this result suggests that many of the county-level gaps in the collection records map may be attributable to spatial biases in tick sampling effort and/or associated reporting apparent as gaps in Figure 2A. In addition, the ensemble map projected an absence of suitable habitat associated with the Appalachian Mountains, an area extending from northern Georgia/eastern Tennessee northeast through eastern Kentucky, western Virginia, and West Virginia, to the southern border of Pennsylvania. The paucity of collection records in associated counties is consistent with this result and suggests that *A. americanum* may not be established in this area. Of the 651 counties categorized as established by Springer and others,[56] 87.6% had a score of 5 in the ensemble model (i.e., all of the optimized models predicted the presence of suitable habitat), and none had a score of 0 (Table 3, Supplemental Table 1). Of the 1,811 counties for which Springer and others[56] found no records of *A. americanum* collection, 74.4% had a score of 0 in the ensemble model and 17.0% had a score of 4 or 5.

TABLE 3

Numbers of counties in the continental United States associated with the categorization scheme used by Springer and others[56] and with consensus habitat suitability scores in our present-day ensemble model and RCP4.5 and RCP8.5 future ensemble predictions. Future predictions are based on future climate projections for 2061–2080. For each of the future ensemble predictions, the numbers of counties with consensus MESS scores in the associated MESS map are also provided

Categorization based on Springer and others[56]	Number of counties	Number of counties with consensus habitat suitability score in present-day ensemble model						–	–	–	–	–	–
Established	651	0	55	3	7	16	570	–	–	–	–	–	–
No records	1,811	1,347	21	66	70	244	63	–	–	–	–	–	–
Reported	647	222	12	13	15	201	184	–	–	–	–	–	–
Total	3,109	1,569	88	82	92	461	817	–	–	–	–	–	–
								Number of counties with consensus MESS score in associated MESS map					
Consensus habitat suitability score in RCP4.5 future ensemble prediction	Number of counties	0	1	2	3	4	5	0	1	2	3	4	5
0	1,233	1,082	38	11	20	26	56	1,151	6	18	10	8	40
1	238	152	9	1	9	28	39	187	4	26	4	5	12
2	335	246	15	6	0	37	31	290	1	15	8	6	15
3	256	50	13	29	10	74	80	156	10	84	2	0	4
4	132	10	2	11	7	32	70	60	5	60	3	2	2
5	915	29	11	24	46	264	541	330	218	335	15	6	11
Total	3,109	1,569	88	82	92	461	817	2,174	244	538	42	27	84
Consensus habitat suitability score in RCP8.5 future ensemble prediction	Number of counties	0	1	2	3	4	5	0	1	2	3	4	5
0	978	792	29	12	24	50	71	810	22	3	4	8	131
1	182	114	4	0	3	33	28	118	8	1	1	5	49
2	213	156	7	0	0	20	30	145	23	4	2	3	36
3	146	80	4	3	1	26	32	63	31	12	13	9	18
4	270	212	6	0	0	10	42	99	128	6	9	5	23
5	1,320	215	38	67	64	322	614	106	252	296	304	83	279
Total	3,109	1,569	88	82	92	461	817	1,341	464	322	333	113	536

MESS = multivariate environmental similarity surface; RCP = representative concentration pathway.

Although there was general agreement between the collection records and ensemble maps, two noteworthy differences were apparent. First, the ensemble map projected suitable habitat in eastern and central Oklahoma and Kansas, areas beyond the apparent western distributional limit suggested by the map of collection records. For Oklahoma, this prediction is supported by a recently published report of tick collection in nearly every county in the state east of the panhandle region.[91] Second, very few if any of the optimized models predicted the presence of suitable habitat north of the 40th northern parallel, a result inconsistent with collection records in areas of the northeast (e.g., New York) and upper Midwest (e.g., Wisconsin) where there is strong evidence that *A. americanum* is in fact established in localized pockets (but generally at relatively low abundance). Some fraction of these northern areas would likely have been identified as suitable habitat had we considered the tick present in counties categorized as reported by Springer and others.[56] Of the 647 counties categorized as reported by Springer and others,[56] 34.3% had a score of 0 in the ensemble model while 59.5% had a score of either 4 (31.1%) or 5 (28.4%) (Table 3, Supplemental Table 1). Maps of the continuous habitat suitability scores generated by each optimized model (Figure 2C–G) showed variation among model predictions, with those of some models being much more spatially conservative (e.g., MARS) than others (e.g., Maxent).

Visualization and evaluation of future predictions. Future ensemble prediction maps suggested a number of changes to the distribution of suitable habitat relative to the present-day ensemble map (Figure 2B). Both RCP4.5 and RCP8.5 future ensemble prediction maps (Figure 3A and B, respectively) projected an expansion of suitable habitat north and east across Iowa, Illinois, Indiana, and Ohio. The northern borders of these states represented the northern limit of expansion in the former scenario, while in the later, suitable habitat extended into central portions of South Dakota, Minnesota,

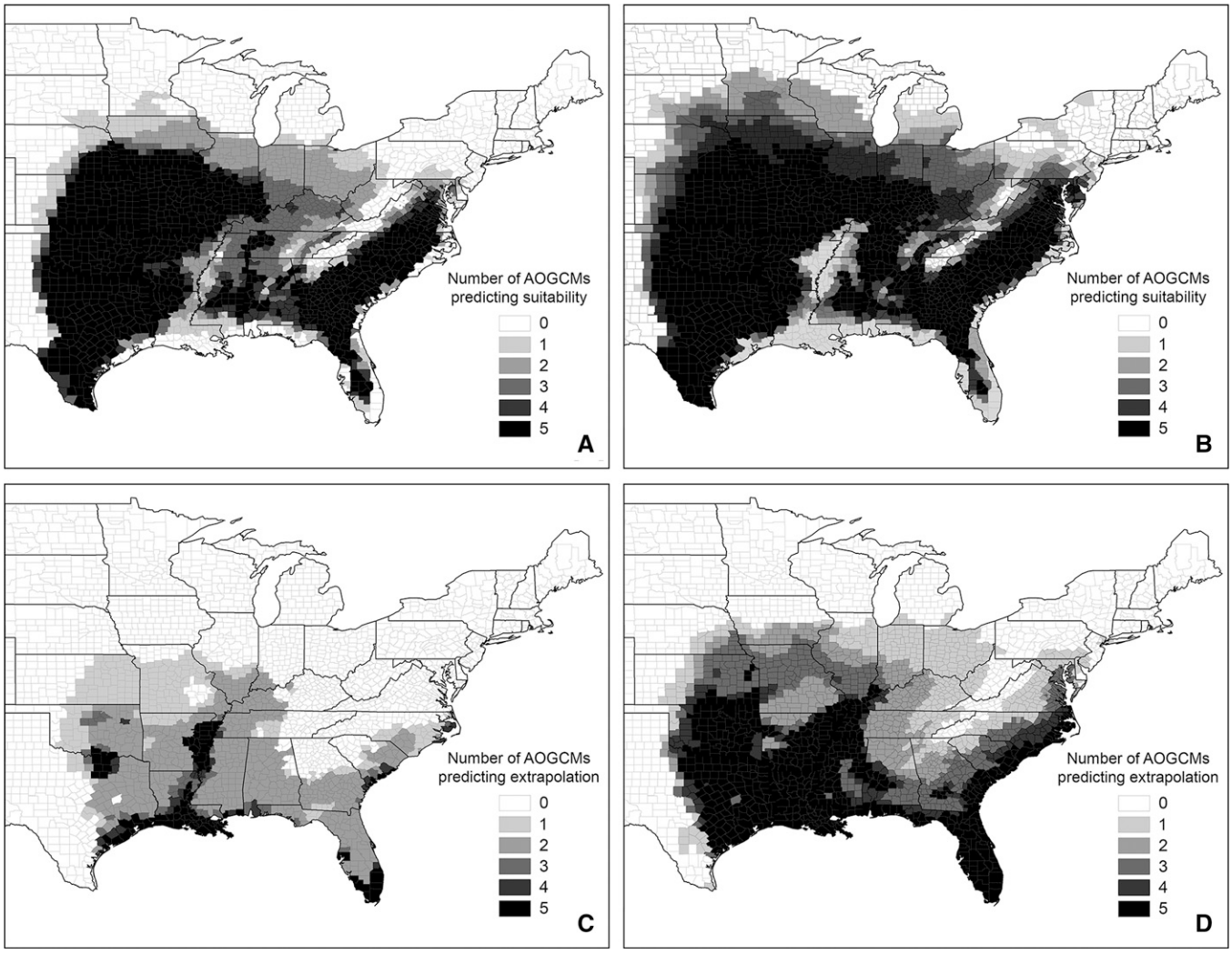

FIGURE 3. Maps depicting predicted future distribution (and associated uncertainty) of habitat climatically suitable for the establishment of *Amblyomma americanum*. Predictions were generated using the optimized present-day distribution model constructed with the GLM algorithm (see Figure 2D) and future climate projections for 2061–2080. Maps of future ensemble predictions depicting consensus habitat suitability scores for (**A**) the RCP4.5 and (**B**) RCP8.5 scenarios are presented above their respective ensemble MESS maps (**C**, **D**). In maps of future ensemble predictions (**A**, **B**), consensus habitat suitability scores indicate the number of the 5 AOGCMs forecasting climate conditions associated with suitable habitat in a given county. In the MESS maps (**C**, **D**), consensus MESS scores indicate the number of the 5 AOGCMs in which climate conditions forecasted in a given county fell outside the historical range of climate conditions observed across all counties.

Wisconsin, and Michigan. East of this region, both future ensemble prediction maps projected suitable habitat in eastern Tennessee and Kentucky and western West Virginia, areas classified as unsuitable in the present-day ensemble model. In eastern areas of the tick's present range, both future ensemble prediction maps projected modest northward expansion of suitable habitat. Only the RCP8.5 ensemble map projected the appearance of suitable habitat across parts of western and central Pennsylvania and in areas of western New York, and neither emissions scenario was associated with the prediction of any suitable habitat north or east of the eastern border of New York. A portion of the band of higher elevation habitat associated with the Appalachian Mountain region remained unsuitable in both future ensemble prediction maps, yet the width of this band was reduced relative to the present-day ensemble model. With the expansion of suitable habitat into northern Virginia, southern Pennsylvania, and portions of West Virginia in the RCP8.5 ensemble map, this band would effectively become an island of unsuitable habitat. Consistent with results of the present-day ensemble model, predictions for both future scenarios forecasted a relatively stable western limit to the distribution of suitable habitat that was roughly coincident with the 100th meridian. Finally, ensemble maps for both future scenarios predicted areas of unsuitable habitat along coastal areas of Florida and the state's panhandle region, southern coastal areas of Alabama, Mississippi, Louisiana, and southeastern Texas, and extending north to varying degrees along the lower Mississippi river valley into northeastern Arkansas and western Tennessee. Because these general areas were identified as suitable habitat in the present-day ensemble model, they could represent locations of future range contraction. It should be noted, however, that many of the associated counties had high MESS scores, indicating high predictive uncertainty due to climatic extrapolation (see below). Of the 1,569 counties with a score of 0 in the present-day ensemble model, 69.0% and 50.5% had the same score in the RCP4.5 and RCP8.5 future ensemble predictions (i.e., none of the five AOGCMs forecasted climatic conditions associated with suitable habitat), respectively, while 2.5% and 27.2% had a score of either 4 or 5 (Table 3, Supplemental Table 1). Of the 817 counties with a score of 5 in the present-day ensemble model, 74.8% and 80.3% had a score of either 4 or 5 in the RCP4.5 and RCP8.5 future ensemble predictions, respectively.

In the ensemble MESS maps for both ensemble predictions (Figure 3C and D), the greatest uncertainty in future predictions was in areas of the south central and southern United States: from eastern Texas and Oklahoma, east across central and southern Mississippi and Alabama to southern Georgia and Florida, and then north along coastal areas of the Carolinas. In the RCP4.5 ensemble MESS map the highest levels of uncertainty (consensus MESS scores of 4 or 5) were concentrated in coastal portions of Gulf coast states (e.g., eastern Texas, Louisiana, Mississippi, Alabama, Florida) and extending along the Louisiana/Mississippi border north through the lower Mississippi river valley to the confluence of northern Arkansas and eastern Tennessee. In the RCP8.5 ensemble MESS map, the total geographic area associated with highest uncertainty was larger, covering most of Oklahoma, eastern Texas, Louisiana, and Arkansas and extending into Midwestern and central states (e.g., eastern Kansas and southeastern Nebraska, northern Missouri, southern Illinois), and further north along the eastern seaboard (e.g., through eastern North Carolina and inland to the base of the Appalachian mountains). In the RCP4.5 ensemble MESS map, 96.5% of counties with an ensemble prediction score of 5 had an ensemble MESS score of 2 or less (i.e., predicted climatic conditions fell outside the historically observed range in 2 or fewer AOGCMs) (Table 3, Supplemental Table 1). In contrast, 50.5% of counties with an RCP8.5 ensemble prediction score of 5 had an ensemble MESS score of 3 or more.

On the basis of the findings of Springer and others[56] *A. americanum* is currently established in 651 counties distributed across 32 states and the DC. According to results of our present-day ensemble model, between 817 counties (all those with a consensus habitat suitability score of 5, 23 states and the DC, 1,360,034 km^2 of total area) and 1,540 counties (all those with consensus habitat suitability score of at least 1, 30 states and the DC, 2,426,368 km^2) are currently associated with suitable habitat. This extent represents between 17% and 31% of the total area of the continental United States. Applying the same delimiters to the RCP4.5 future ensemble prediction, between 915 counties (19 states, 1,520,078 km^2) and 1,876 counties (29 states and the DC, 2,808,752 km^2) were forecasted to experience climatic conditions associated with suitable habitat. This would represent a range of between 20% and 36% of the total area of the continental United States. By comparison, between 1,320 counties (23 states and the DC, 2,027,839 km^2) and 2,131 counties (31 states and the DC, 3,279,726 km^2) were forecasted to experience climatic conditions associated with suitable habitat by the RCP8.5 future ensemble prediction (between 26% and 42% of the total area of the continental United States). It must be noted, however, that values of these forecasted statistics are likely overestimates for at least two reasons. First, the county-level scale of the analyses assumes that conditions will be homogeneous across entire counties. In reality, it is highly likely that within counties classified as suitable, only a fraction of the total county area will actually be associated with suitable habitat. Second, summary statistics generated for the future ensemble predictions could be made more conservative by incorporating uncertainty information from the MESS maps. As the most extreme example, when counties associated with climatic extrapolation in any one of the five AOGCMs (consensus MESS score of 1 or more) were excluded from the tallies associated with the RCP4.5 future ensemble prediction, the range of counties forecasted to have suitable climatic conditions shrank to between 330 (13 states, 516,490 km^2) and 1,023 (25 states and the DC, 1,371,458 km^2). Because the RCP8.5 scenario is associated with more extreme climate change, the effects of this MESS filtering on summary statistics were even more pronounced: the range of climatically suitable counties shrank to between 106 (six state, 231,564 km^2) and 531 (22 states, 944,772 km^2).

DISCUSSION

Despite being a major nuisance biter and serving as the primary vector for multiple pathogens of public health significance, the pattern of distribution of *A. americanum* within the continental United States has received relatively little attention. This contrasts sharply with *Ixodes scapularis*, the primary vector associated with Lyme disease in eastern North America and a species whose distribution has been the focus of considerable interest and study.[24,57,92–95] Developing a well-resolved

distribution map of the range of *A. americanum* represents an important first step for both guiding future research on tick ecology and biogeography as well as raising awareness of *A. americanum*-associated diseases, particularly in more northerly areas where the tick has become established relatively recently. Using an ensemble approach to account for uncertainty across modeling algorithms, we generated a climate-based ensemble model that can be used to predict the present-day distribution of locations within the continental United States associated with climatic conditions suitable for the establishment of *A. americanum*. With the exception of a relatively high elevation region associated with the Appalachian Mountains, our analyses suggested that suitable habitat effectively extends eastward to the Atlantic coast from the 100th meridian and southward from the 40th parallel. Our analyses further suggested that humidity during summer months is the primary determinant of habitat suitability. On the basis of two different climate change scenarios (RCP 4.5 and 8.5) and projected conditions for the period 2061–2080, our future ensemble predictions included a relatively stable western limit to the distribution of suitable habitat, an expansion of suitable habitat north into the Upper Midwest and east into the Ohio River Valley and western Pennsylvania, and potential disappearance of suitable habitat in areas along the Gulf coast and in the lower Mississippi river valley.

Mean vapor pressure in July was the only climate predictor included in all five optimized models and had the highest explanatory power. In reducing the original set of 66 climate predictors to arrive at the nine variable reduced set, mean vapor pressure in July had the highest value of deviance explained and was strongly correlated with mean vapor pressure in all months from April through October (inclusive, correlation coefficient ≥ 0.9), mean temperature of warmest quarter (Bio10, correlation coefficient = 0.89), and annual mean temperature (Bio1, correlation coefficient = 0.84). These correlations are not surprising given that vapor pressure is strongly dependent on and positively related to temperature, particularly as it nears saturation (i.e., when RH is high) (Supplemental Material 2). Results of our present-day modeling therefore indicate that humidity (vapor pressure) and temperature, especially from late spring through early autumn, are disproportionately important in defining the fundamental (here, climatic) niche and distribution of *A. americanum*. The minimum threshold value for mean vapor pressure in July identified by the response curves of our optimized models is approximately equal to values observed around the 100th meridian, with vapor pressure decreasing to the west (Supplemental Figure 1). Further, values of mean vapor pressure in July identified as optimal by our models are only observed in areas of the southeastern United States where *A. americanum* is highly abundant. Humidity exerts strong effects on the activity patterns and survival of hard ticks of many species.[23,96–100] Laboratory studies involving nymphal and adult *A. americanum* have estimated the critical equilibrium activity (water vapor activity [%RH/100] at which ticks can remain adequately hydrated by absorbing water vapor from the air) to be between 0.80 and 0.88, indicating relatively high sensitivity to desiccation and dependence on a moisture-rich environment.[101–103] Oviposition, egg-hatching rates, and larval survival and molting success in *A. americanum* are also sensitive to and require high humidity (approximately $\geq 70\%$).[104] The effects of humidity on tick mortality are likely to be greatest during the period of peak host-seeking activity when ticks spend more time away from favorable microclimate conditions found in the leaf litter or close to the soil. For Lone star ticks, this period spans April–July for adults, May–August for nymphs, and July–September for larvae.[105] As such, the summer months represent the portion of the year when all three life stages are actively seeking hosts and may be most vulnerable to desiccation stress. In modeling the distribution of *A. americanum* within Missouri, Brown and others[106] found that RH in July was a significant predictor of nymphal and adult abundance. Similarly, James and others[34] modeled the climatic niche of the American dog tick (*Dermacentor variabilis*) and found a strong effect of normalized difference vegetation index in July, which they posited is an indicator of humidity levels on the ground. It should be noted that in our analyses we modeled vapor pressure using atmospheric measurements. Humidity experienced by ticks in microhabitats associated with the ground and leaf litter should in general be correlated with but higher than atmospheric humidity.

Although all of the other eight climate predictor variables included in our present-day modeling had very limited explanatory power, two warrant mention. Mean temperature of the driest quarter (Bio9) and annual precipitation (Bio12) were both included in four of the five models and had the second and third highest explanatory power behind mean vapor pressure in July, respectively. The response curves for Bio9 varied among optimized models and there were no clear, consistent, relationships with habitat suitability. This apparently equivocal result may be due in part to the fact that the period of the year that constitutes the driest quarter varies geographically (Supplemental Figure 2). Specifically, Missouri, eastern Oklahoma, and northwestern Arkansas, areas that are all highly suitable for *A. americanum*, experience their driest quarter in winter, whereas other highly suitable states such as eastern Arkansas, Louisiana, Alabama, and Mississippi experience their driest quarter in the summer. Therefore, the modest positive slope observed at approximately 17.5°C in the response curves of three of four models (Figure 1) likely reflects increased suitability for *A. americanum* in areas of the southeast that experience warmer late-spring to early-autumn temperatures and also experience high RH (Supplemental Figure 1). With the exception of the Maxent model, habitat suitability appears to change little in response to temperature in areas where the driest months occurs in the winter (e.g., where mean temperature of the driest quarter is less than 5°C), a finding that might suggest that the insulating effects of snow cover could result in winter temperatures having a negligible effect on establishment. In contrast to Bio9, there seemed to be relatively consistent evidence of an asymptotic relationship between habitat suitability and annual precipitation (Bio12), with positive increases in suitability up to a peak between 1,200 and 1,400 mm. Two of the models indicated decreases in suitability at higher levels of precipitation while two indicated no effect of additional precipitation on suitability. Similar to the pattern for mean vapor pressure in July, a dramatic decline in annual precipitation west of the 100th meridian likely contributes to conditions that are prohibitively dry for tick establishment (Supplemental Figure 1).

The five optimized models varied both in their structure (number and identity of climatic predictor variables included) and their spatial predictions of habitat suitability across the continental United States. Geographic variation among models

could be generally characterized based on the predicted likelihood and spatial extent of suitable habitat in three geographic regions: 1) a core area of distribution in south central and southeastern regions where *A. americanum* is known to occur in high abundance, 2) areas west of the 100th meridian where *A. americanum* is unlikely to be currently established, and 3) areas of the northeast and upper Midwest located north of the 40th parallel into which the range of *A. americanum* may be expanding.[56]All five optimized models included vapor pressure in July and predicted high habitat suitability within the core area. The optimized BRT model included the fewest number of climatic predictor variables (two) and predicted suitable habitat almost exclusively within this core area. In contrast,, the optimized GLM and MARS models both included three climatic predictor variables and predicted moderately suitable habitat in the northeast and upper Midwest. In addition to vapor pressure in July, both of these models also included annual precipitation (Bio12). The MARS model was the only one of the five to predict extensive areas of low habitat suitability west of the 100th meridian. The optimized Maxent and RF models both included all nine climate predictor variables. The former predicted broad areas of relatively high habitat suitability within the northeast and upper Midwest, and patchy areas of low habitat suitability west of the 100th meridian. By comparison, the latter had the most spatially conservative predictions. Locations with the highest predicted habitat suitability largely coincided with counties categorized as established by Springer and others,[56] with scattered clusters of areas of considerably lower predicted suitability interspersed among them.

Our present-day models (the five individual optimized models and the ensemble model created from them) performed well in predicting the presence of suitable habitat in the core area of the distribution of *A. americanum*.[56] Extending to the coast from the 100th meridian in the west and the 40th parallel in the north and excluding higher elevation regions associated with the Appalachian Mountains, this area is consistent with the spatial distribution of *A. americanum* collected as part of a large-scale field study of *I. scapularis*[92] and with qualitative, continental-scale distribution maps produced to date for the Lone star tick.[48,107,108] The area is also roughly coincident with the predicted and observed spatial distribution of *E. chaffeensis* (in white-tailed deer) (*Odocoileus virginianus*),[109–112] a zoonotic pathogen for which *A. americanum* is the principle vector.[107] The distribution of human cases of ehrlichiosis, a disease caused primarily by *E. chaffeensis*, also falls largely within this area. For example, of the 4,619 cases of confirmed human infection by *E. chaffeensis* reported to the U.S. Centers for Disease Control and Prevention from 2008 through 2012, 62% were associated with residents of seven states located centrally within our predicted distribution of suitable *A. americanum* habitat: Oklahoma, Missouri, Arkansas, Kentucky, Tennessee, Virginia, North Carolina).[113–117] Finally, the distribution of suitable habitat is also consistent with general biogeographic patterns identified by studies of other Ixodid ticks. For example, Diuk-Wasser and others[92] reported the 100th meridian as the western distributional limit of *I. scapularis* and also failed to collect any individuals of that species or *D. variabilis* at multiple sites in the Appalachian Mountains. In creating a county-level map of records of *I. scapularis* collections, Dennis and others.[57] found the species to be essentially absent from the Appalachian region.

In contrast to results associated with the tick's core area of distribution, the present-day and ensemble models generally failed to predict suitable habitat in areas north of the 40th parallel even though *A. americanum* is known to be established in localized pockets in the northeast and upper Midwest (e.g., areas of New York, Connecticut, Rhode Island, Maine, Wisconsin).[56] A post hoc analysis that separately compared predictions among counties north and south of the 40th parallel revealed that on average, the sensitivity of individual optimized models (proportion of established counties classified as presence locations) was 97% in the south but only 46% in the north. Similarly, 97% of established counties in the south received a consensus habitat suitability score of 4 or 5 in the present-day ensemble model compared with only 33% of northern established counties. A total of 64% of northern established counties were only identified as suitable habitat by the optimized RF model. The low sensitivity of our models in the north could be attributable to true biological variation. For example, habitat suitability in northern areas might be driven by different climatic conditions or to a greater extent by biotic factors than in the south. Alternatively, the results might reflect the relatively low and spatially localized surveillance efforts in the north. Given the broad spatial scale of our models, the influence of a small number of northern established counties on model predictions was likely swamped by that of the large number of southern counties. This imbalance could be addressed through either greater surveillance in northern areas to identify additional counties where *A. americanum* is established and/or the construction of finer scale, localized models that focus on these northern regions. Such efforts seem warranted given the widely held belief that the range of *A. americanum* is expanding northward.

Model predictions about the spatial distribution of suitable habitat are likely robust in terms of climatic factors. In our analyses, we considered a diverse suite of climate predictors including variables that are known to have strong effects on tick growth, survival, and/or reproduction and that have been identified as important contributors in modeled distributions of other tick species.[118] In addition, we used the most updated and empirically robust range map for *A. americanum* that included numerous known established locations distributed across the full geographic and climatic extent of the presumed extant range of the species.[56] Finally, we generated predictions using an ensemble approach that combined results of multiple algorithms that varied in the number and identity of the climate predictors included and in the modeled relationships between those variables and habitat suitability. Nevertheless, while our analyses have likely defined the climatic niche of *A. americanum* reasonably well, there are at least four limitations that could contribute to disparities between our results and the actual present-day distribution (~realized niche) of the Lone star tick. First, our analyses did not consider the distribution of host species that represent the tick's food source. Although *A. americanum* is known to feed on a variety of species of reptiles, birds, and small- and medium-sized mammals, the white-tailed deer (*O. virginianus*) is considered the tick's principle wildlife host.[54] Large-scale changes in the distribution and abundance of *O. virginianus* within the continental United States caused primarily by hunting have been linked to concomitant effects on the biogeography of species of ticks including *A. americanum*.[54] Second, our analyses did not directly incorporate information on the distribution of vegetation known to be important to Lone star tick ecology. Specifically, the relative abundance of *A. americanum* is highest

within young, second-growth woodland habitats where dense understory vegetation creates microclimatic conditions optimal for ticks survival.[54] As with white-tailed deer, reductions in the extent of woodland habitat in the United States caused by anthropogenic deforestation and agricultural development have been correlated with changes in the distribution of *A. americanum*.[54] Although we recognize that host availability and vegetation are important in determining tick establishment, neither variable was included in our analyses because present-day distributions are not of suitable quality or desired spatial resolution and/or future distributions are poorly defined. Third, colonization of a specific location by ticks will require both the presence of suitable habitat as well as successful dispersal to that location. Dispersal of ticks occurs primarily through movement of hosts, the majority of which range across relatively limited geographic extents (e.g., < 100 km). Although ticks of many species can travel longer distances while feeding on birds,[119] these migrants are generally reproductively immature larvae or nymphs. Establishment of ticks in a new location would require either the dispersal of one or more gravid adult female ticks that lay eggs following arrival, or of multiple immature stages with post-arrival survival, contact, and reproduction. Finally, because our analyses had a broad geographic extent overall, our results are spatially coarse at the level of individual counties. Mean climatic conditions for any given county, calculated from one or a few associated climate data grid cells, are an obvious oversimplification of the range of microclimates present within that county. In reality, it is likely that a portion of every county classified in its entirety as suitable habitat by our analyses would not support *A. americanum* populations given climatic conditions at smaller spatial scales.

Future ensemble predictions based on conditions associated with both of the simulated climate change scenarios (Supplemental Figures 3–5) forecasted northward expansion of suitable habitat into areas of the Upper Midwest and northeast into the Ohio River Valley. This result in directionally consistent with observed and modeled changes in the distribution of *I. scapularis*, which is most abundant in parts of its range associated with states in Northeast and upper Midwest and is expanding northward into areas of eastern and central Canada.[28,32,37] In our results, the extent of predicted expansion of suitable habitat was greater in the RCP8.5 scenario, which is associated with higher emissions and more extreme warming. Maps for both future ensembles suggested considerable increases in the proportion of suitable habitat in Iowa, Illinois, Indiana, and Ohio. With greater warming, southern and central portions of South Dakota, Minnesota, Wisconsin, and Michigan are also likely to increase in suitability. These changes are almost certainly driven by warming and the accompanying changes in humidity, particularly during spring and summer months. As the climate warms and average saturation vapor pressure increases concomitantly, higher vapor pressure (humidity) conditions will become more common, particularly during warmer times of year.[74] In contrast, extensive northward expansion of suitable habitat into northeastern states was not predicted under either scenario, with no suitable habitat forecasted east of New York in either model. Extreme precipitation events have become more frequent in the northeastern United States in recent decades,[120] and precipitation is forecasted to increase in the northeastern United States under future climate scenarios.[121] This could render habitat unsuitable by increasing the frequency and/or degree of water saturation that results in inundation. Predictions for both scenarios forecasted essentially no westward extension of suitable habitat beyond the 100th meridian, suggesting that this longitude may represent a relatively stable biogeographic boundary for *A. americanum*. Distance from the Gulf of Mexico moisture source and increases in elevation beginning at this longitude likely render areas to the west inhospitable due to insufficient moisture. Finally, both future ensemble predictions suggested the potential for range contraction in coastal areas of Florida, Alabama, Mississippi, Louisiana, and eastern Texas, as well as in the region of the lower Mississippi river valley extending from southern Louisiana to the Tennessee/Arkansas border. As in the northeastern United States, loss of suitable habitat in these areas appears to be rooted in future increases in precipitation to levels that are inhospitable for ticks due to inundation. It should be noted, however, that the intermediate habitat suitability scores predicted for these areas by the optimized present-day GLM model (Figure 2D) suggest that they are already associated with suboptimal climatic conditions at the present time. Further, because these areas were associated with relatively high consensus scores in both MESS maps, this prediction of range contraction should be interpreted with caution.

The Lone star tick is increasingly recognized as a vector species of significant public health importance in North America. Predictions about future distributional changes of *A. americanum* highlight areas where public health information campaigns could be initiated proactively and where field studies of tick ecology (e.g., investigating physiology at range limits, invasion dynamics) might be conducted. In addition, our results complement and build upon those of Springer and others[56] by providing a contiguous, county-level representation of the present-day spatial distribution of areas associated with habitat climatically suitable for the establishment of *A. americanum* within the continental United States. Together, results of these present-day habitat suitability models and future ensemble predictions provide a foundation upon which more comprehensive studies of *A. americanum* biogeography (e.g., incorporating information about other aspects of tick ecology including vegetation associations, host distributions, and/or dispersal) can be based.

Received May 4, 2015. Accepted for publication June 9, 2015.

Published online July 27, 2015.

Note: Supplemental data, table, and figures appear at www.ajtmh.org.

Acknowledgments: We thank K. S. King and K. A. Medley for their involvement in and contributions to early stages of the project, and C. B. Talbert for downloading and preparing the Daymet data for analyses. Comments from H. R. Sofaer and an anonymous reviewer improved the clarity of the manuscript and are greatly appreciated.

Financial support: This work was partially supported by the U.S. Centers for Disease Control and Prevention, the U.S. Geological Survey, and the National Center for Atmospheric Research, which is sponsored by the National Science Foundation.

Disclaimer: None of the authors have any relationships, or have received any support, that would constitute a conflict of interest relative to the material presented herein. Any use of trade, firm, or product names is for descriptive purposes only and does not imply endorsement by the U.S. Government.

Authors' addresses: Yuri P. Springer and Rebecca J. Eisen, Centers for Disease Control and Prevention, Division of Vector-Borne Diseases, Fort Collins, CO, E-mails: yurispringer@gmail.com and dyn2@cdc.gov. Catherine S. Jarnevich, U.S. Geological Survey, Fort Collins,

CO, E-mail: jarnevichc@usgs.gov. David T. Barnett, National Ecological Observatory Network, Inc., Boulder, CO, E-mail: dbarnett@neoninc.org. Andrew J. Monaghan, National Center for Atmospheric Research, Boulder, CO, E-mail: monaghan@ucar.edu.

REFERENCES

1. Parmesan C, 2006. Ecological and evolutionary responses to recent climate change. *Annu Rev Ecol Evol Syst 37:* 637–669.
2. Chen IC, Hill JK, Ohlemueller R, Roy DB, Thomas CD, 2011. Rapid range shifts of species associated with high levels of climate warming. *Science 333:* 1024–1026.
3. Parmesan C, Yohe G, 2003. A globally coherent fingerprint of climate change impacts across natural systems. *Nature 421:* 37–42.
4. Root TL, Price JT, Hall KR, Schneider SH, Rosenzweig C, Pounds JA, 2003. Fingerprints of global warming on wild animals and plants. *Nature 421:* 57–60.
5. Deutsch CA, Tewksbury JJ, Huey RB, Sheldon KS, Ghalambor CK, Haak DC, Martin PR, 2008. Impacts of climate warming on terrestrial ectotherms across latitude. *Proc Natl Acad Sci USA 105:* 6668–6672.
6. Paaijmans KP, Heinig RL, Seliga RA, Blanford JI, Blanford S, Murdock CC, Thomas MB, 2013. Temperature variation makes ectotherms more sensitive to climate change. *Glob Change Biol 19:* 2378–2380.
7. Gage KL, Burkot TR, Eisen RJ, Hayes EB, 2008. Climate and vectorborne diseases. *Am J Prev Med 35:* 436–450.
8. Githeko AK, Lindsay SW, Confalonieri UE, Patz JA, 2000. Climate change and vector-borne diseases: a regional analysis. *Bull World Health Organ 78:* 1136–1147.
9. Sutherst RW, 2004. Global change and human vulnerability to vector-borne diseases. *Clin Microbiol Rev 17:* 136–173.
10. Altizer S, Ostfeld RS, Johnson PTJ, Kutz S, Harvell CD, 2013. Climate change and infectious diseases: from evidence to a predictive framework. *Science 341:* 514–519.
11. Epstein PR, 2005. Climate change and human health. *N Engl J Med 353:* 1433–1436.
12. Harvell CD, Mitchell CE, Ward JR, Altizer S, Dobson AP, Ostfeld RS, Samuel MD, 2002. Climate warming and disease risks for terrestrial and marine biota. *Science 296:* 2158–2162.
13. Rohr JR, Dobson AP, Johnson PTJ, Kilpatrick AM, Paull SH, Raffel TR, Ruiz-Moreno D, Thomas MB, 2011. Frontiers in climate change-disease research. *Trends Ecol Evol 26:* 270–277.
14. Rosenthal J, 2009. Climate change and the geographic distribution of infectious diseases. *EcoHealth 6:* 489–495.
15. Patz JA, Campbell-Lendrum D, Holloway T, Foley JA, 2005. Impact of regional climate change on human health. *Nature 438:* 310–317.
16. Jongejan F, Uilenberg G, 2004. The global importance of ticks. *Parasitology 129:* S3–S14.
17. Randolph SE, 2001. The shifting landscape of tick-borne zoonoses: tick-borne encephalitis and *Lyme borreliosis* in Europe. *Philos Trans R Soc Lond B Biol Sci 356:* 1045–1056.
18. Kuehn BM, 2013. CDC estimates 300,000 U.S. cases of Lyme disease annually. *JAMA 310:* 1110–1110.
19. Bock R, Jackson L, De Vos A, Jorgensen W, 2004. Babesiosis of cattle. *Parasitology 129:* S247–S269.
20. McLeod R, Kristjanson P, 1999. *TickCost Project—Economic Impacts of Ticks and Tick-Borne Diseases to Livestock in Africa, Asia, and Australia*. Final report of joint esys/ILRI/ACIAR. Nairobi, Kenya: International Livestock Research Institute.
21. Needham GR, Teel PD, 1991. Off-host physiological ecology of Ixodid ticks. *Annu Rev Entomol 36:* 659–681.
22. Sauer JR, Hair JA, 1986. *Morphology, Physiology, and Behavioral Biology of Ticks*. Chichester, United Kingdom: Ellis Horwood Limited, 510.
23. Sonenshine DE, Roe RM, 2014. *Biology of Ticks*. Oxford, United Kingdom: Oxford University Press.
24. Brownstein JS, Holford TR, Fish D, 2003. A climate-based model predicts the spatial distribution of the Lyme disease vector *Ixodes scapularis* in the United States. *Environ Health Perspect 111:* 1152–1157.
25. Ogden NH, Bigras-Poulin M, O'Callaghan CJ, Barker IK, Lindsay LR, Maarouf A, Smoyer-Tomic KE, Waltner-Toews D, Charron D, 2005. A dynamic population model to investigate effects of climate on geographic range and seasonality of the tick *Ixodes scapularis. Int J Parasitol 35:* 375–389.
26. Eisen L, 2008. Climate change and tick-borne diseases: a research field in need of long-term empirical field studies. *Int J Med Microbiol 298:* 12–18.
27. Jaenson TGT, Jaenson DGE, Eisen L, Petersson E, Lindgren E, 2012. Changes in the geographical distribution and abundance of the tick *Ixodes ricinus* during the past 30 years in Sweden. *Parasit Vectors 5:* 1–15.
28. Ogden NH, Maarouf A, Barker IK, Bigras-Poulin M, Lindsay LR, Morshed MG, O'Callaghan CJ, Ramay F, Waltner-Toews D, Charron DF, 2006. Climate change and the potential for range expansion of the Lyme disease vector *Ixodes scapularis* in Canada. *Int J Parasitol 36:* 63–70.
29. Ogden NH, Lindsay LR, Morshed M, Sockett PN, Artsob H, 2009. The emergence of Lyme disease in Canada. *CMAJ 180:* 1221–1224.
30. Randolph SE, 2010. To what extent has climate change contributed to the recent epidemiology of tick-borne diseases? *Vet Parasitol 167:* 92–94.
31. Leger E, Vourc'h G, Vial L, Chevillon C, McCoy KD, 2013. Changing distributions of ticks: causes and consequences. *Exp Appl Acarol 59:* 219–244.
32. Ogden NH, Mechai S, Margos G, 2013. Changing geographic ranges of ticks and tick-borne pathogens: drivers, mechanisms and consequences for pathogen diversity. *Front Cell Infect Microbiol 3:* 46.
33. Medlock JM, Hansford KM, Bormane A, Derdakova M, Estrada-Pena A, George JC, Golovljova I, Jaenson TGT, Jensen JK, Jensen PM, Kazimirova M, Oteo JA, Papa A, Pfister K, Plantard O, Randolph SE, Rizzoli A, Santos-Silva MM, Sprong H, Vial L, Hendrickx G, Zeller H, Van Bortel W, 2013. Driving forces for changes in geographical distribution of *Ixodes ricinus* ticks in Europe. *Parasit Vectors 6:* 1–11.
34. James A, Burdett C, McCool M, Fox A, Riggs P, 2015. The geographic distribution and ecological preferences of the American dog tick, *Dermacentor variabilis* (Say), in the USA. *Med Vet Entomol 29:* 178–188.
35. Porretta D, Mastrantonio V, Amendolia S, Gaiarsa S, Epis S, Genchi C, Bandi C, Otranto D, Urbanelli S, 2013. Effects of global changes on the climatic niche of the tick *Ixodes ricinus* inferred by species distribution modelling. *Parasit Vectors 6:* 271.
36. Leighton PA, Koffi JK, Pelcat Y, Lindsay LR, Ogden NH, 2012. Predicting the speed of tick invasion: an empirical model of range expansion for the Lyme disease vector *Ixodes scapularis* in Canada. *J Appl Ecol 49:* 457–464.
37. Ogden NH, St-Onge L, Barker IK, Brazeau S, Bigras-Poulin M, Charron DF, Francis CM, Heagy A, Lindsay LR, Maarouf A, Michel P, Milord F, O'Callaghan CJ, Trudel L, Thompson RA, 2008. Risk maps for range expansion of the Lyme disease vector, *Ixodes scapularis*, in Canada now and with climate change. *Int J Health Geogr 7:* 24.
38. Guisan A, Thuiller W, 2005. Predicting species distribution: offering more than simple habitat models. *Ecol Lett 8:* 993–1009.
39. Elith J, Leathwick JR, 2009. Species distribution models: ecological explanation and prediction across space and time. *Annu Rev Ecol Evol Syst 40:* 677–697.
40. Pearson RG, Dawson TP, 2003. Predicting the impacts of climate change on the distribution of species: are bioclimate envelope models useful? *Glob Ecol Biogeogr 12:* 361–371.
41. Hutchinson GE, 1957. Population studies—animal ecology and demography - concluding remarks. *Cold Spring Harb Symp Quant Biol 22:* 415–427.
42. Grinnell J, 1917. Field tests of theories concerning distributional control. *Am Nat 51:* 115–128.
43. Araujo MB, Guisan A, 2006. Five (or so) challenges for species distribution modelling. *J Biogeogr 33:* 1677–1688.
44. Araujo MB, Peterson AT, 2012. Uses and misuses of bioclimatic envelope modeling. *Ecology 93:* 1527–1539.
45. Thomas CD, 2010. Climate, climate change and range boundaries. *Divers Distrib 16:* 488–495.
46. Araujo MB, New M, 2007. Ensemble forecasting of species distributions. *Trends Ecol Evol 22:* 42–47.

47. Heikkinen RK, Luoto M, Araujo MB, Virkkala R, Thuiller W, Sykes MT, 2006. Methods and uncertainties in bioclimatic envelope modelling under climate change. *Prog Phys Geogr 30:* 751–777.
48. Hair JA, Howell DE, 1970. Lone star ticks: their biology and control in Ozark recreation areas. *Okla State Univ Agr Expt Sta Bul B-679:* 47.
49. Bolte JR, Hair JA, Fletcher J, 1970. White-tailed deer mortality following tissue destruction induced by Lone star ticks. *J Wildl Manage 34:* 546–552.
50. Barnard DR, 1985. Injury thresholds and production loss functions for the Lone star tick, *Amblyomma americanum* (Acari, *Ixodidae*), on pastured, preweaner beef cattle, *Bos taurus. J Econ Entomol 78:* 852–855.
51. Childs JE, Paddock CD, 2003. The ascendancy of *Amblyomma americanum* as a vector of pathogens affecting humans in the United States. *Annu Rev Entomol 48:* 307–337.
52. Goddard J, Varela-Stokes AS, 2009. Role of the Lone star tick, *Amblyomma americanum* (L.), in human and animal diseases. *Vet Parasitol 160:* 1–12.
53. Mixson TR, Campbell SR, Gill JS, Ginsberg HS, Reichard MV, Schulze TL, Dasch GA, 2006. Prevalence of *Ehrlichia, Borrelia,* and *Rickettsial* agents in *Amblyomma americanum* (Acari: *Ixodidae*) collected from nine states. *J Med Entomol 43:* 1261–1268.
54. Paddock CD, Yabsley MJ, 2007. *Ecological Havoc, the Rise of White-Tailed Deer, and the Emergence of Amblyomma americanum—Associated Zoonoses in the United States.* Wildlife and Emerging Zoonotic Diseases: The Biology, Circumstances and Consequences of Cross-Species Transmission. Heidelberg, Germany: Springer Berlin, 289–324.
55. Savage HM, Godsey MS, Lambert A, Panella NA, Burkhalter KL, Harmon JR, Lash RR, Ashley DC, Nicholson WL, 2013. First detection of Heartland virus (Bunyaviridae: Phlebovirus) from field collected arthropods. *Am J Trop Med Hyg 89:* 445–452.
56. Springer YP, Eisen L, Beati L, James AM, Eisen RJ, 2014. Spatial distribution of counties in the continental United States with records of occurrence of *Amblyomma americanum* (Ixodida: *Ixodidae*). *J Med Entomol 51:* 342–351.
57. Dennis DT, Nekomoto TS, Victor JC, Paul WS, Piesman J, 1998. Reported distribution of *Ixodes scapularis* and *Ixodes pacificus* (Acari: *Ixodidae*) in the United States. *J Med Entomol 35:* 629–638.
58. Hijmans RJ, Cameron SE, Parra JL, Jones PG, Jarvis A, 2005. Very high resolution interpolated climate surfaces for global land areas. *Int J Climatol 25:* 1965–1978.
59. Gray J, Dautel H, Estrada-Peña A, Kahl O, Lindgren E, 2009. Effects of climate change on ticks and tick-borne diseases in Europe. *Interdiscip Perspect Infect Dis 2009:* 593232.
60. Eisen RJ, Lane RS, Fritz CL, Eisen L, 2006. Spatial patterns of Lyme disease risk in California based on disease incidence data and modeling of vector-tick exposure. *Am J Trop Med Hyg 75:* 669–676.
61. Thornton PE, Thornton MM, Mayer BW, Wilhelmi N, Wei Y, Devarakonda R, Cook RB, 2014. *Daymet: Daily Surface Weather Data on a 1-km Grid for North America; Version 2.* Oak Ridge, TN: Oak Ridge National Laboratory (ORNL) Distributed Active Archive Center.
62. Thornton PE, Thornton MM, Mayer BW, Wilhelmi N, Wei Y, Devarakonda R, Cook R, 2012. *Daymet: Daily Surface Weather on a 1 km Grid for North America, 1980–2008.* Oak Ridge, TN: Oak Ridge National Laboratory (ORNL) Distributed Active Archive Center for Biogeochemical Dynamics (DAAC).
63. Moore SM, Eisen RJ, Monaghan A, Mead P, 2014. Meteorological influences on the seasonality of Lyme disease in the United States. *Am J Trop Med Hyg 90:* 486–496.
64. Taylor KE, Stouffer RJ, Meehl GA, 2012. An overview of CMIP5 and the experiment design. *Bull Am Meteorol Soc 93:* 485–498.
65. Knutti R, Masson D, Gettelman A, 2013. Climate model genealogy: generation CMIP5 and how we got there. *Geophys Res Lett 40:* 1194–1199.
66. Gent PR, Danabasoglu G, Donner LJ, Holland MM, Hunke EC, Jayne SR, Lawrence DM, Neale RB, Rasch PJ, Vertenstein M, Worley PH, Yang ZL, Zhang MH, 2011. The community climate system model version 4. *J Clim 24:* 4973–4991.
67. Giorgetta MA, Jungclaus J, Reick CH, Legutke S, Bader J, Bottinger M, Brovkin V, Crueger T, Esch M, Fieg K, Glushak K, Gayler V, Haak H, Hollweg HD, Ilyina T, Kinne S, Kornblueh L, Matei D, Mauritsen T, Mikolajewicz U, Mueller W, Notz D, Pithan F, Raddatz T, Rast S, Redler R, Roeckner E, Schmidt H, Schnur R, Segschneider J, Six KD, Stockhause M, Timmreck C, Wegner J, Widmann H, Wieners KH, Claussen M, Marotzke J, Stevens B, 2013. Climate and carbon cycle changes from 1850 to 2100 in MPI-ESM simulations for the Coupled Model Intercomparison Project phase 5. *J Adv Model Earth Sy 5:* 572–597.
68. Collins WJ, Bellouin N, Doutriaux-Boucher M, Gedney N, Halloran P, Hinton T, Hughes J, Jones CD, Joshi M, Liddicoat S, Martin G, O'Connor F, Rae J, Senior C, Sitch S, Totterdell I, Wiltshire A, Woodward S, 2011. Development and evaluation of an Earth-System model-HadGEM2. *Geosci Model Dev 4:* 1051–1075.
69. Voldoire A, Sanchez-Gomez E, Melia DSY, Decharme B, Cassou C, Senesi S, Valcke S, Beau I, Alias A, Chevallier M, Deque M, Deshayes J, Douville H, Fernandez E, Madec G, Maisonnave E, Moine MP, Planton S, Saint-Martin D, Szopa S, Tyteca S, Alkama R, Belamari S, Braun A, Coquart L, Chauvin F, 2013. The CNRM-CM5.1 global climate model: description and basic evaluation. *Clim Dyn 40:* 2091–2121.
70. Bi DH, Dix M, Marsland SJ, O'Farrell S, Rashid HA, Uotila P, Hirst AC, Kowalczyk E, Golebiewski M, Sullivan A, Yan HL, Hannah N, Franklin C, Sun ZA, Vohralik P, Watterson I, Zhou XB, Fiedler R, Collier M, Ma YM, Noonan J, Stevens L, Uhe P, Zhu HY, Griffies SM, Hill R, Harris C, Puri K, 2013. The ACCESS coupled model: description, control climate and evaluation. *Aust Meteorol Oceanogr J 63:* 41–64.
71. Moss RH, Edmonds JA, Hibbard KA, Manning MR, Rose SK, Van Vuuren DP, Carter TR, Emori S, Kainuma M, Kram T, 2010. The next generation of scenarios for climate change research and assessment. *Nature 463:* 747–756.
72. Riahi K, Rao S, Krey V, Cho C, Chirkov V, Fischer G, Kindermann G, Nakicenovic N, Rafaj P, 2011. RCP 8.5—A scenario of comparatively high greenhouse gas emissions. *Clim Change 109:* 33–57.
73. Thomson AM, Calvin KV, Smith SJ, Kyle GP, Volke A, Patel P, Delgado-Arias S, Bond-Lamberty B, Wise MA, Clarke LE, 2011. RCP4. 5: a pathway for stabilization of radiative forcing by 2100. *Clim Change 109:* 77–94.
74. Willett KM, Jones PD, Gillett NP, Thorne PW, 2008. Recent changes in surface humidity: development of the HadCRUH dataset. *J Clim 21:* 5364–5383.
75. Held IM, Soden BJ, 2000. Water vapor feedback and global warming. *Annu Rev Energy Environ 25:* 441–475.
76. Wood S, 2006. *Generalized Additive Models: An Introduction with R.* Boca Raton, FL: CRC press.
77. Dormann CF, Elith J, Bacher S, Buchmann C, Carl G, Carre G, Marquez JRG, Gruber B, Lafourcade B, Leitao PJ, Munkemuller T, McClean C, Osborne PE, Reineking B, Schroder B, Skidmore AK, Zurell D, Lautenbach S, 2013. Collinearity: a review of methods to deal with it and a simulation study evaluating their performance. *Ecography 36:* 27–46.
78. Morisette JT, Jarnevich CS, Holcombe TR, Talbert CB, Ignizio D, Talbert MK, Silva C, Koop D, Swanson A, Young NE, 2013. VisTrails SAHM: visualization and workflow management for species habitat modeling. *Ecography 36:* 129–135.
79. Elith J, Leathwick JR, Hastie T, 2008. A working guide to boosted regression trees. *J Anim Ecol 77:* 802–813.
80. McCullagh P, Nelder JA, 1989. *Generalized Linear Models.* London, United Kingdom: Chapman and Hall.
81. Friedman JH, 1991. Multivariate adaptive regression splines. *Ann Stat 19:* 1–67.
82. Phillips SJ, Dudík M, 2008. Modeling of species distributions with Maxent: new extensions and a comprehensive evaluation. *Ecography 31:* 161–175.
83. Breiman L, 2001. Random forests. *Mach Learn 45:* 5–32.
84. Dormann CF, Purschke O, Marquez JRG, Lautenbach S, Schroder B, 2008. Components of uncertainty in species

distribution analysis: a case study of the great grey shrike. *Ecology 89:* 3371–3386.
85. Liu CR, White M, Newell G, 2013. Selecting thresholds for the prediction of species occurrence with presence-only data. *J Biogeogr 40:* 778–789.
86. Manel S, Williams HC, Ormerod SJ, 2001. Evaluating presence–absence models in ecology: the need to account for prevalence. *J Appl Ecol 38:* 921–931.
87. Fielding AH, Bell JF, 1997. A review of methods for the assessment of prediction errors in conservation presence/absence models. *Environ Conserv 24:* 38–49.
88. Allouche O, Tsoar A, Kadmon R, 2006. Assessing the accuracy of species distribution models: prevalence, Kappa and the True skill statistic (TSS). *J Appl Ecol 43:* 1223–1232.
89. Jiménez-Valverde A, Lobo JM, Hortal J, 2008. Not as good as they seem: the importance of concepts in species distribution modelling. *Divers Distrib 14:* 885–890.
90. Marmion M, Parviainen M, Luoto M, Heikkinen RK, Thuiller W, 2009. Evaluation of consensus methods in predictive species distribution modelling. *Divers Distrib 15:* 59–69.
91. Barrett AW, Noden BH, Gruntmeir JM, Holland T, Mitcham JR, Martin JE, Johnson EM, Little SE, 2015. County scale distribution of *Amblyomma americanum* (Ixodida: *Ixodidae*) in Oklahoma: addressing local deficits in tick maps based on passive reporting. *J Med Entomol 52:* 269–273.
92. Diuk-Wasser MA, Gatewood AG, Cortinas MR, Yaremych-Hamer S, Tsao J, Kitron U, Hickling G, Brownstein JS, Walker E, Piesman J, Fish D, 2006. Spatiotemporal patterns of host-seeking *Ixodes scapularis* nymphs (Acari: *Ixodidae*) in the United States. *J Med Entomol 43:* 166–176.
93. Diuk-Wasser MA, Vourc'h G, Cislo P, Hoen AG, Melton F, Hamer SA, Rowland M, Cortinas R, Hickling GJ, Tsao JI, Barbour AG, Kitron U, Piesman J, Fish D, 2010. Field and climate-based model for predicting the density of host seeking nymphal *Ixodes scapularis*, an important vector of tick-borne disease agents in the eastern United States. *Glob Ecol Biogeogr 19:* 504–514.
94. Fish D, Howard C, 1999. Methods used for creating a national Lyme disease risk map. *MMWR 48:* 21–24.
95. Estrada-Peña A, 2002. Increasing habitat suitability in the United States for the tick that transmits Lyme disease: a remote sensing approach. *Environ Health Perspect 110:* 635.
96. Berger KA, Ginsberg HS, Gonzalez L, Mather TN, 2014. Relative humidity and activity patterns of *Ixodes scapularis* (Acari: *Ixodidae*). *J Med Entomol 51:* 769–776.
97. Berger KA, Ginsberg HS, Dugas KD, Hamel LH, Mather TN, 2014. Adverse moisture events predict seasonal abundance of Lyme disease vector ticks (*Ixodes scapularis*). *Parasit Vectors 7:* 181.
98. Vail SG, Smith G, 1998. Air temperature and relative humidity effects on behavioral activity of blacklegged tick (Acari: *Ixodidae*) nymphs in New Jersey. *J Med Entomol 35:* 1025–1028.
99. Perret JL, Guigoz E, Rais O, Gern L, 2000. Influence of saturation deficit and temperature on *Ixodes ricinus* tick questing activity in a *Lyme borreliosis*-endemic area (Switzerland). *Parasitol Res 86:* 554–557.
100. Stafford KC, 1994. Survival of immature *Ixodes scapularis* (Acari, *Ixodidae*) at different relative humidities. *J Med Entomol 31:* 310–314.
101. Yoder JA, Benoit JB, 2003. Water vapor absorption by nymphal lone star tick, *Amblyomma americanum* (Acari: *Ixodidae*), and its ecological significance. *Int J Acarol 29:* 259–264.
102. Hair JA, Sauer JR, Durham KA, 1975. Water balance and humidity preference in three species of ticks. *J Med Entomol 12:* 37–47.
103. Sauer JR, Hair JA, 1971. Water balance in Lone star tick (Acarina-*Ixodidae*)—effects of relative humidity and temperature on weight changes and total water content. *J Med Entomol 8:* 479–485.
104. Lancaster JL, McMillan HL, 1955. The effects of relative humidity on the Lone star tick. *J Econ Entomol 48:* 338–339.
105. Kollars TM, Oliver JH, Durden LA, Kollars PG, 2000. Host associations and seasonal activity of *Amblyomma americanum* (Acari: *Ixodidae*) in Missouri. *J Parasitol 86:* 1156–1159.
106. Brown HE, Yates KF, Dietrich G, MacMillan K, Graham CB, Reese SM, Helterbrand WS, Nicholson WL, Blount K, Mead PS, Patrick SL, Eisen RJ, 2011. An acarologic survey and *Amblyomma americanum* distribution map with implications for tularemia risk in Missouri. *Am J Trop Med Hyg 84:* 411–419.
107. Yabsley MJ, 2010. Natural History of *Ehrlichia chaffeensis*: vertebrate hosts and tick vectors from the United States and evidence for endemic transmission in other countries. *Vet Parasitol 167:* 136–148.
108. Bishopp FC, Trembley HL, 1945. Distribution and hosts of certain North American ticks. *J Parasitol 31:* 1–54.
109. Yabsley MJ, Wimberly MC, Stallknecht DE, Little SE, Davidson WR, 2005. Spatial analysis of the distribution of *Ehrlichia chaffeensis*, causative agent of human monocytotropic ehrlichiosis, across a multi-state region. *Am J Trop Med Hyg 72:* 840–850.
110. Wimberly MC, Baer AD, Yabsley MJ, 2008. Enhanced spatial models for predicting the geographic distributions of tick-borne pathogens. *Int J Health Geogr 7:* 1–15.
111. Yabsley MJ, Dugan VG, Stallknecht DE, Little SE, Lockhart JM, Dawson JE, Davidsoni WR, 2003. Evaluation of a prototype *Ehrlichia chaffeensis* surveillance system using white-tailed deer (*Odocoileus virginianus*) as natural sentinels. *Vector Borne Zoonotic Dis 3:* 195–207.
112. Dugan VG, Yabsley MJ, Tate CM, Mead DG, Munderloh UG, Herron MJ, Stallknecht DE, Little SE, Davidson WR, 2006. Evaluation of White tailed deer (*Odocoileus virginianus*) as natural sentinels for *Anaplasma phagocytophilum. Vector Borne Zoonotic Dis 6:* 192–207.
113. Centers for Disease Control and Prevention, 2010. Summary of notifiable diseases—United States, 2008. *MMWR 57:* 1–94.
114. Centers for Disease Control and Prevention, 2011. Summary of notifiable diseases—United States, 2009. *MMWR 58:* 1–100.
115. Centers for Disease Control and Prevention, 2012. Summary of notifiable diseases—United States, 2010. *MMWR 59:* 1–111.
116. Centers for Disease Control and Prevention, 2013. Summary of notifiable diseases—United States, 2011. *MMWR 60:* 1–118.
117. Centers for Disease Control and Prevention, 2014. Summary of notifiable diseases—United States, 2012. *MMWR 61:* 1–122.
118. Ostfeld RS, Brunner JL, 2015. Climate change and *Ixodes* tick-borne diseases of humans. *Philos Trans R Soc Lond B Biol Sci 370:* 20140051.
119. Scott JD, Anderson JF, Durden LA, 2012. Widespread dispersal of *Borrelia burgdorferi*-infected ticks collected from songbirds across Canada. *J Parasitol 98:* 49–59.
120. Guilbert J, Betts AK, Rizzo DM, Beckage B, Bomblies A, 2015. Characterization of increased persistence and intensity of precipitation in the northeastern United States. *Geophys Res Lett 42:* 1888–1893.
121. Rawlins M, Bradley RS, Diaz H, 2012. Assessment of regional climate model simulation estimates over the northeast United States. *J Geophys Res Atmos 117:* D23112.